Water isotope diffusion rates from the NorthGRIP ice core for the last 16,000 years - glaciological and paleoclimatic implications.

V. Gkinis[1,2], S. B. Simonsen[1,3], S. L. Buchardt[1], J. W. C. White[2], and B. M. Vinther[1]

[1]Centre for Ice and Climate, Niels Bohr Institute, University of Copenhagen, Juliane Maries Vej 30, DK-2100 Copenhagen, Denmark

[2]Institute for Alpine and Arctic Research, University of Colorado, Boulder, 1560 30th Street Boulder, CO 80303 USA

[3]Div. of Geodynamics, DTU space National Space Institute, Elektrovej, Build. 327, Kgs. Lyngby, Denmark

arXiv:1404.4201v3 [physics.geo-ph] 17 Mar 2015

***Abstract*—A high resolution (0.05 m) water isotopic record (δ^{18}O) is available from the NorthGRIP ice core. In this study we look into the water isotope diffusion history as estimated by the spectral characteristics of the δ^{18}O time series covering the last 16,000 years. Based on it we infer a temperature history signal for the site. We use a water isotope diffusion model coupled to a steady-state densification model in order to infer the temperature signal from the site, assuming the accumulation and strain rate history as estimated using the GICC05 layer counted chronology and a Dansgaard–Johnsen ice flow model. The necessary corrections regarding ice diffusion and the discretized sampling of the dataset are also described. The temperature reconstruction accurately captures the timing and magnitude of the Bølling–Allerød and Younger Dryas transitions. A Holocene climatic optimum is seen between 7 and 9 ky b2k with an apparent cooling trend thereafter. Our temperature estimate for the Holocene climatic optimum, point to a necessary adjustment of the total thinning function indicating that the ice flow model overestimates the accumulation rates by about 10% at 8 ky b2k. This result, is also supported by recent gas isotopic fractionation studies proposing a similar reduction for glacial conditions. Finally, the record presents a climatic variability over the Holocene spanning millennial and centennial scales with a profound cooling occurring at approximately 4000 years b2k. The new reconstruction technique is able to provide past temperature estimates by overcoming the potential issues apparent in the use of the classical δ^{18}O slope method, while it can in the same time resolve temperature signals at low and high frequencies.**

I. Introduction

Polar ice core records provide some of the most detailed views of past environmental changes up to 800,000 years before present, in a large part via proxy data such as the water isotopic composition and embedded chemical impurities. One of the most important features of ice cores as climate archives, is their continuity and the potential for high temporal resolution. The relevance of this type of paleoclimate data archive is high within the context of the study of Earth's climate system and thus the possibility to predict future climate changes.

The isotopic signature of polar precipitation, commonly expressed through the δ notation [1] (Epstein, 1953; Mook, 2000) is related to the temperature gradient between the evaporation and condensation site (Dansgaard, 1964) and has so far been used as a proxy for the temperature of the cloud at the time of condensation (Jouzel and Merlivat, 1984; Jouzel et al., 1997; Johnsen et al., 2001). Previous studies (Johnsen et al., 1989; Lorius et al., 1969) have reported a linear relationship between the isotopic signal of polar precipitation and the temperature at the precipitation site. For Greenland sites and present conditions, Johnsen et al. (2001) used a linear relationship between the mean annual surface temperature and the mean annual isotopic value of snow described as:

$$\delta^{18}\mathrm{O} = 0.67 \cdot T(^{\circ}\mathrm{C}) - 13.7\ ‰. \quad (1)$$

Assuming that the isotope sensitivity of 0.67 $‰\mathrm{K}^{-1}$ in Eq.(1) (hereafter "spatial slope" ζ_s) holds for different

[1] Isotopic abundances are typically reported as deviations of a sample's isotopic ratio relative to that of a reference water (e.g. VSMOW) expressed through the δ notation: $\delta^i = \frac{{}^i\mathrm{R}_{\mathrm{sample}}}{{}^i\mathrm{R}_{\mathrm{SMOW}}} - 1\,[‰]$ where ${}^2\mathrm{R} = \frac{{}^2\mathrm{H}}{{}^1\mathrm{H}}$ and ${}^{18}\mathrm{R} = \frac{{}^{18}\mathrm{O}}{{}^{16}\mathrm{O}}$

climatic regimes (as glacial conditions and inter-stadial events) one can reconstruct the temperature history of an ice core site based on the measured δ^{18}O profile.

The validity of the temperature reconstruction based on ζ_s was questioned when studies based on borehole temperature inversion (Cuffey et al., 1994; Johnsen et al., 1995; Dahl Jensen et al., 1998) and gas isotopic fractionation studies (Severinghaus et al., 1998; Severinghaus and Brook, 1999; Lang et al., 1999; Schwander et al., 1997; Landais et al., 2004) were developed. The aforementioned studies drew the following conclusions regarding the isotopic thermometer. First, the isotopic slope is not constant with time. Second, during glacial conditions the spatial slope presents an isotopic sensitivity higher than the sensitivity suggested by the borehole inversion and gas isotopic studies. As a result, reconstructions of past temperatures based on the water isotope signal, should assess the sensitivity of the δ^{18}O to temperature for different climatic regimes, thus inferring the "temporal slope" ζ_t.

The main reasons that drive the fluctuations of ζ_t with time are not precisely determined yet. Changes of the vapor source location and temperature, the possible presence of an atmospheric inversion over the precipitation site, microphysical cloud processes affecting the in–cloud phase changes, as well as effects related to the seasonality of the precipitation, have previously been proposed as possible causes of this behavior (Jouzel et al., 1997). Furthermore, Vinther et al. (2009) showed how changes of the ice sheet geometry affect the elevation of ice core sites and can create isotopic artifacts, thus "masking" the Holocene climatic optimum signal from ice core records. The complications emerging from the variable nature of ζ_t, have possibly also resulted in the isotopic signal pointing towards a climatically stable Holocene epoch. A very low signal to noise ratio is observed in the δ^{18}O signal of almost every deep ice core from the Greenland ice divide. This observation contradicts with studies that indicate that the Holocene epoch has not been as stable as previously thought and likely significant climatic changes have occurred at high latitude sites (Denton and Karlen, 1973; Bond et al., 2001). More recently, and based on combined δ^{15}N and δ^{40}Ar gas analysis on the GISP2 ice core Kobashi et al. (2011) suggested temperature variations up to 3 K during the last 4,000 years. The impacts of these changes are believed to have been significant for the evolution of past human civilizations (Dalfes et al., 1997; deMenocal, 2001; Weiss and Bradley, 2001).

An alternative way to extract temperature information from the water isotopic signal, is to look into its spectral properties. The isotopic signal experiences attenuation via a molecular diffusion process that happens after snow deposition, during the stage of firn densification. Information on this process is contained in the spectral characteristics of the δ^{18}O signal. We work here along the lines of previously published work by Johnsen (1977), Johnsen et al. (2000) and Simonsen et al. (2011) presenting a technique that is based on the spectral analysis of the δ^{18}O signal only, thus not requiring dual isotope measurements of both δ^{18}O and δD as in Simonsen et al. (2011). An estimate of the densification process is vital for this type of study and can be carried out in various ways (Herron and Langway, 1980; Alley et al., 1982; Schwander et al., 1997; Goujon et al., 2003), with each approach posing its own uncertainty levels, implementation characteristics and challenges. The technique yields actual firn temperatures and thus overcomes many of the issues of the traditional δ^{18}O thermometer based on the "temporal slope" ζ_t.

II. The water isotope diffusion - densification model

We will outline here the theory of water isotope diffusion in firn and ice. Almost exclusively, the formulations used here are based on the work presented in Johnsen (1977) and Johnsen et al. (2000) and the experimental work of Jean-Baptiste et al. (1998) and Van der Wel et al. (2011).

The diffusion of water isotopes in firn is a process that occurs after the deposition of precipitation. It is a molecular exchange process taking place in the vapor phase and it is driven by isotopic gradients existing along the firn column. As the densification of firn continues, the diffusion process slows down until it ceases at pore close off. Assuming a coordinate system fixed on a sinking layer of firn, the process can be described mathematically with Fick's second law accounting for layer thinning as:

$$\frac{\partial \delta}{\partial t} = D\left(t\right) \frac{\partial^2 \delta}{\partial z^2} - \dot{\varepsilon}_z\left(t\right) z \, \frac{\partial \delta}{\partial z} \ . \tag{2}$$

Here, $D\left(t\right)$ is the diffusivity coefficient and $\dot{\varepsilon}_z\left(t\right)$ the vertical strain rate. Use of Fourier integrals yields the solution to Eq.(2) as the convolution of the initial isotopic signal $\delta\left(z,0\right)$ with a Gaussian filter of standard deviation σ:

$$\mathcal{G} = \frac{1}{\sigma\sqrt{2\pi}} \, e^{\frac{-z^2}{2\sigma^2}} \ , \tag{3}$$

The isotopic signal $\delta\left(z,t\right)$ will then be given by

$$\delta\left(z,t\right) = \mathcal{S}\left(t\right) \frac{1}{\sigma\sqrt{2\pi}} \int_{-\infty}^{+\infty} \delta\left(z,0\right) \exp\left\{\frac{-\left(z-u\right)^2}{2\sigma^2}\right\} \mathrm{d}u \ . \tag{4}$$

Here $\mathcal{S}(t)$ is the total thinning the layer has experienced during the time interval $t = 0 \rightarrow t = t'$ due to the ice flow and equal to:

$$\mathcal{S}\left(t'\right) = e^{\int_0^{t'} \dot{\varepsilon}_z(t)\mathrm{d}t} \quad . \tag{5}$$

The standard deviation term σ of the Gaussian filter, commonly referred to as diffusion length, represents the mean displacement of a water molecule along the z-axis and can be calculated as (Johnsen, 1977):

$$\frac{\mathrm{d}\sigma^2}{\mathrm{d}t} - 2\,\dot{\varepsilon}_z(t)\,\sigma^2 = 2D(t) \quad . \tag{6}$$

In the firn the simple strain rate can be assumed

$$\dot{\varepsilon}_z\left(t\right) = -\frac{\mathrm{d}\rho}{\mathrm{d}t}\,\frac{1}{\rho}. \tag{7}$$

Combining Eq.(6) and Eq.(7) and substituting the independent variable t with the density ρ, we can calculate the quantity σ^2 provided an expression of the diffusivity $D\left(\rho\right)$ (see SOM), a density profile for the site and its adjoint age are estimated. The expression we finally get for the diffusion length is (see SOM for a more detailed derivation):

$$\sigma^2\left(\rho\right) = \frac{1}{\rho^2}\int_{\rho_o}^{\rho} 2\rho^2 \left(\frac{\mathrm{d}\rho}{\mathrm{d}t}\right)^{-1} D(\rho)\;\mathrm{d}\rho, \tag{8}$$

where with ρ_o we symbolize the surface density. In this study we used the empirical steady-state densification model by Herron and Langway (1980) (H–L model hereafter), according to which:

$$\frac{\mathrm{d}\rho(z)}{\mathrm{d}t} = K(T)A^{\vartheta}\frac{\rho_{\mathrm{ice}} - \rho(z)}{\rho_{\mathrm{ice}}}. \tag{9}$$

Here $K(T)$ is a temperature dependent Arrhenius–type densification rate coefficient, A is the annual accumulation rate (here in $\mathrm{kgm^{-2}yr^{-1}}$) and ϑ is a factor that determines the effect of the accumulation rate during the different stages of the densification. For a better insight on those parameters the reader is referred to Herron and Langway (1980).

At the close–off depth, the process of diffusion in the vapor phase ceases. After $\rho \geq \rho_{\mathrm{ice}}$, self diffusion takes place in the solid phase. For the temperature dependence of the diffusivity we use an Arrhenius type equation as (Ramseier, 1967; Johnsen et al., 2000):

$$D_{ice} = 9.2 \cdot 10^{-4} \cdot \exp\left(-\frac{7186}{T}\right)\mathrm{m^2 s^{-1}}. \tag{10}$$

In order to calculate the quantity σ_{ice} we start from Eq.(6) and use D_{ice} as the diffusivity parameter,

$$\frac{\mathrm{d}\sigma_{ice}^2}{\mathrm{d}t} - 2\,\dot{\varepsilon}_z(t)\,\sigma_{ice}^2 = 2D_{ice}(t)\,. \tag{11}$$

The solution for Eq.(11) yields (see SOM):

$$\sigma_{ice}^2\left(t'\right) = S\left(t'\right)^2 \int_0^{t'} 2D_{ice}(t)\,S(t)^{-2}\;\mathrm{d}t \tag{12}$$

For a further discussion on the ice diffusion coefficient the reader is referred to the SOM.

In conclusion, if with σ_{firn}^2 we symbolize the firn diffusion length as estimated by performing the integration in Eq.(8) from the surface density ρ_o to the close–off density ρ_{co} and expressed in ice equivalent length, then the total diffusion length at a depth z_i will be:

$$\sigma_i^2\left(z\right) = \left[S(z)\sigma_{\mathrm{firn}}(z)\right]^2 + \sigma_{\mathrm{ice}}^2(z) \tag{13}$$

In this study, for the estimation of σ_{ice}^2 we use the temperature profile from the borehole of the NorthGRIP core (Dahl-Jensen et al., 2003) and assume a steady state condition.

In Fig. 1 the quantities σ_i, σ_{ice}, σ_{firn} and $S(z)\sigma_{\mathrm{firn}}$ are illustrated for typical modern day conditions at NorthGRIP. These parameters are only approximately representative of the modern NorthGRIP conditions and chosen as such, solely for the purpose of illustration.

III. Estimation of the diffusion length based on high resolution δ^{18}O datasets

The transfer function for the Gaussian filter in Eq. (3) will be given by its Fourier transform, which is itself a Gaussian and equal to

$$\mathfrak{F}[\mathcal{G}_{\mathrm{cfa}}(z)] = \hat{\mathcal{G}}_{\mathrm{cfa}} = e^{\frac{-k^2\sigma^2}{2}} \quad , \tag{14}$$

where $k = 2\pi/\Delta$ and Δ is the sampling resolution of the δ^{18}O time series (Abramowitz and Stegun, 1964). Harmonics with an initial amplitude Γ_0 and wavenumber k will be attenuated to a final amplitude Γ_s as described in Eq.(15):

$$\Gamma_s = \Gamma_0 e^{\frac{-k^2\sigma^2}{2}} \tag{15}$$

Based on the latter, one can describe the behavior of the power spectrum of the isotopic time series that has been subjected to the firn diffusion process, assuming that at the time of deposition the power spectral density shows a white noise behavior. For a time series that is sampled at resolution equal to Δ and presenting a noise level described by $\eta\left(k\right)$ the power spectral density will be described as:

$$P_s = P_\sigma + \left|\hat{\eta}\left(k\right)\right|^2 \tag{16}$$

$$\text{where}\;\; P_\sigma = P_0 e^{-k^2\sigma^2},\;\; k = 2\pi f \;\text{ and }\; f \in \left[0,\;\frac{1}{2\Delta}\right] \tag{17}$$

From Eq.(16, 17) one can see that the estimation of the diffusion length σ benefits from time series sampled at a high resolution Δ and presenting a low noise level $\eta(k)$.

We obtain an estimate $\hat{P}_s$ of the power spectral density density P_s by using Burg's spectral estimation method assuming a μ-order autoregressive (AR-μ) process (Kay and Marple, 1981; Hayes, 1996). On a sliding window with a length of 500 points (25 m), we apply the algorithm described in Andersen (1974). We obtain an estimate for the diffusion length σ^2, by minimizing the misfit between P_s and $\hat{P}_s$ in the least squares sense. An example of an estimated spectrum and the inferred model is given in Fig. 2. Additional information on the spectral and σ^2 estimation can be found in the SOM.

IV. Inferring temperatures from the estimated diffusion lengths

Let us assume that the total diffusion length value $\widehat{\sigma}_i^2$ at depth z_i is estimated from the power spectral density and a combination of firn densification and flow model parameters as well as an estimate of past accumulation rates is known. The first step towards obtaining a temperature T_i is to account for the artifactual diffusion that occurs due to the finite sampling scheme. We require that the transfer function of a rectangular filter with width equal to Δ, is equal to the transfer function of a Gaussian filter with diffusion length σ_{dis}^2. This results in:

$$\sigma_{dis}^2 = \frac{2\Delta^2}{\pi^2} \log\left(\frac{\pi}{2}\right). \tag{18}$$

Then, the sampling diffusion length is subtracted from $\hat{\sigma}_i^2$ in the Gaussian sense as:

$$\sigma_i^2 = \widehat{\sigma}_i^2 - \sigma_{\text{dis}}^2. \tag{19}$$

Combining Eq.(13, 19) we get

$$\sigma_{\text{firn}}^2 = \frac{\widehat{\sigma}_i^2 - \sigma_{\text{dis}}^2 - \sigma_{\text{ice}}^2}{S(z)^2}. \tag{20}$$

The result of this calculation describes the data based diffusion length of the layer under consideration at the close–off depth in m ice eq.

A model based calculation of the diffusion length at the close–off depth can be obtained that will allow the calculation of the temperature T. Central to this calculation is Eq. 8 where $\rho = \rho_{\text{co}}$ and the integration takes place from the surface density ρ_o to the close–off density ρ_{co}. The primed notation is used for the model based diffusion length estimate as $\sigma_{\text{firn}}^{\prime 2}$. Additional to the temperature T, the model also requires a value for the accumulation rate parameter A. Our accumulation rate estimates are based on the combined information from the ice flow model and the estimate of the annual layer thickness, available from the GICC05 chronology (see section V-B). The temperature estimation uses the Newton-Raphson method in order to find the roots of the term:

$$\underbrace{\left(\frac{\rho_{\text{co}}}{\rho_{\text{ice}}}\right)^2 \sigma^2\left(\rho = \rho_{\text{co}}, T(z), A(z)\right)}_{\sigma_{\text{firn}}^{\prime 2}} - \sigma_{\text{firn}}^2. \tag{21}$$

The computation is summarized in the block diagram in Fig. 5.

V. The NorthGRIP diffusion length based temperature history

A. The high resolution δ^{18}O NorthGRIP record

The NorthGRIP ice core was drilled at $75.10\ ^{\circ}\text{N}$, $42.32\ ^{\circ}\text{W}$ at an elevation of 2,917 m, to a depth of 3,085 m and extending back to 123,000 years (NGRIP members, 2004). A high resolution record of $\delta^{18}\text{O}$ is available from this ice core with a resolution of $\Delta = 0.05$ m. Stable isotope $\delta^{18}\text{O}$ analysis were performed at the stable isotope laboratory of the University of Copenhagen using a SIRA10 isotope ratio mass spectrometer with an adjacent $\text{CO}_2 - \text{H}_2\text{O}$ isotopic equilibration system. The combined uncertainty of the system is 0.06 ‰. The high resolution $\delta^{18}\text{O}$ record down to 1700 m is presented in Fig. 2.

B. Dating - accumulation and strain rate history

The NorthGRIP ice core has been dated by manual counting of annual layers down to 60 ka, as a part of the Greenland Ice Core Chronology 2005 (GICC05) (Vinther et al., 2006; Rasmussen et al., 2006; Andersen et al., 2006; Svensson et al., 2008). In this study, a combination of the GICC05 estimated annual layer thickness $\lambda(z)$ and a thinning function $S(z)$ inferred by an ice flow model provides an accumulation rate history $A(z)$ for the site. We use a Dansgaard-Johnsen (hereafter D–J model) type 1–D ice flow model (Dansgaard and Johnsen, 1969) with basal melting and sliding. The model is inverted in a Monte–Carlo fashion allowing estimation of the ice flow parameters and constrained by measured depth–age horizons. The values inferred from the model for the present day accumulation rate, basal melting and the kink height are $A_{\text{modern}} = 0.189\ \text{m y}^{-1}$ (ice equiv.), $b = 7.5\ 10^{-3}\ \text{m y}^{-1}$ and $\mathcal{H} = 1620\ \text{m}$ respectively. In Fig. 3, we present the annual layer thickness together with the estimated thinning function and the accumulation rate. Note how the $S(z)$ varies linearly with depth. This is a result of the D–J flow model that requires the horizontal velocity to be constant from the surface until the kink height of $\mathcal{H} = 1620\text{m}$ (1465 m depth).

C. The diffusion length record for NorthGRIP

For the calculation of the diffusion length profile we follow the power spectral estimation approach as described in section III and section 4 in the SOM. In order to investigate the stability of the spectral estimation technique we vary the value of the order μ of the AR filter in the interval $[40, 80]$. This results in 41 estimates of the diffusion length for every depth, providing an estimate of the stability of the power spectral estimation as well as the variance of the diffusion length estimation.

In Fig. 4, we present the result of the this estimation representing the value of $\widehat{\sigma}_i^2$ together with its adjoint variance (top panel in Fig. 4. We also show the result of the discrete sampling, ice flow thinning and ice diffusion correction representing the value of σ^2_{firn}. This is the data-based diffusion length value we use in order to infer the temperature of the record using the computation scheme described in section IV and illustrated in Fig. 5. Based on a sensitivity study described in detail in section 5 of the SOM we estimate the uncertainty of the reconstruction to be approximately 2.5 K (1σ).

VI. Discussion

A. General picture

Based on a diffusion length estimation for the last 16,000 years we reconstructed a temperature history for the NorthGRIP site. In Fig. 6 we present the temperature reconstruction after applying two sharp low–pass filters with a cut–offs at 200 and 1000 y. The reconstruction stops at 225y b2k, a time that corresponds approximately to the present close–off depth. The diffusion based reconstruction, results in a mean temperature between 250 and 350 y b2k of 241.4 K (-31.7 C). This is a reasonable estimate within the prescribed error bars, considering the modern temperature at the NorthGRIP site of $-31.5^{\circ}\mathrm{C}$ (NGRIP members, 2004). Additionally the temperature history presents an obvious Holocene optimum at ≈ 8ky b2k. However, a temperature gradient of 10 K between the Holocene optimum and the present time is not supported by any previous study and is likely unrealistic. We assess this issue in more detail in section VI-B

The record shows two prominent transitions from colder to warmer climatic conditions at $\approx$ 14.7ky and 11.7ky respectively resembling the Bølling–Allerød (BA) and Younger Dryas (YD) oscillations. Based on our reconstruction, the amplitudes of those events are found to be 10.7 ± 1.5K and 7 ± 1.5 K respectively. These results are in line with $\delta^{15}\mathrm{N}$ studies from the summit of Greenland as presented in Severinghaus et al. (1998); Grachev and Severinghaus (2005) and Severinghaus and Brook (1999). In our reconstruction, the absolute temperature right before the beginning of the warming of the YD termination is calculated to be 232 ± 2.3 K, a temperature that is significantly higher than the suggested 227 K in Severinghaus et al. (1998).

When calculated using the "classical" isotope thermometer and assuming a constant sensitivity of $0.67\ ‰\mathrm{K}^{-1}$, the magnitudes of these oscillations are underestimated by almost a factor of two. To overcome this problem, Johnsen et al. (1995) tuned the isotope sensitivity using the low resolution borehole inferred temperature history (Cuffey et al., 1995; Dahl Jensen et al., 1998) and assuming a quadratic relationship between temperature and the $\delta^{18}\mathrm{O}$ signal. With this in mind and considering that our result is based on the $\delta^{18}\mathrm{O}$ signal itself, we find our conclusions to be relevant within the discussion regarding the overall validity and eventually the importance of the isotope thermometer.

At approximately 8.5 ky b2k we observe a strong cooling event (≈ 5 K) that lasts about 500 years. Similar paleoclimatic signals indicating widespread cooler/drier conditions have been reported from regions of the North Atlantic (Andrews et al., 1999; Risebrobakken et al., 2003; Rohling and Palike, 2005) as well as monsoon areas (Gasse, 2000; Haug et al., 2001; Gupta et al., 2003; Wang et al., 2005). The magnitude and age of the event resemble those of the 8.2k event observed in the $\delta^{18}\mathrm{O}$ signal of Greenland ice cores (Alley et al., 1997). Even though the 8.2k event could possibly be seen as part of a more general climate instability (Ellison et al., 2006), it would be speculative to propose that the North Atlantic freshening mechanism that likely triggered the 8.2k event was the same for the longer cooling event we observe here.

B. Proposed thinning function correction

Considering the above features of our temperature reconstruction, we can comment that apart from the Holocene optimum discrepancy and warm glacial, the general characteristics of the signal are in line with the synthesized picture we have for the Greenland summit temperature history over the last 16ky years. This picture is based on a variety of methods and proxies, most prominently the gas isotopic fractionation $\delta^{15}\mathrm{N}$ studies and the borehole inversion technique. Additionally, our technique seems to overcome some of the problems of the classical interpretation of the $\delta^{18}\mathrm{O}$ signal, caused by the variable nature of the isotope temperature sensitivity with time.

With that in mind, we hereby propose that the observed Holocene optimum discrepancy is due to an

inaccurate correction for the total thinning $S(z)$ as described in Eq.(13) and illustrated in Fig. 4. In order to account for this effect we correct σ_i^2 with a modified thinning function $S'(z)$. We tune $S'(z)$ such that the obtained temperature at 8ky b2k is ≈ 3 K higher than the temperature at 225y b2k, in line with Dahl Jensen et al. (1998) and Johnsen et al. (1995, 2001). This is obtained by assuming a linearly varying thinning function with respect to depth and setting $S'(z = 2100) = 0.28$. The temperature reconstruction that utilizes the proposed modified thinning function is presented in Fig. 6.

By adopting this correction we do not impose any change in the higher frequencies of the temperature signal. As a result the magnitudes of the BA and the YD transitions remain unaltered. The same applies for the 8.5k cooling event as well as the rest of the observed Holocene variability. Additionally, the thinning correction has an impact on the inferred temperature of the Younger – Dryas stadial, resulting in a temperature of 227.5 ± 2.3 K. With this updated estimate, we achieve an agreement well within the 1σ uncertainty when compared to Severinghaus et al. (1998).

Here we assume that the use of the modified thinning function $S'(z)$ should not imply a change on the layer counted GICC05 chronology and the profile of annual layer thickness $\lambda(z)$. Hence, the proposed change requires a reduction of the inferred accumulation rates. In Fig. 7, we present the old and proposed scenarios for the thinning function and accumulation rates. We use the primed notation for the proposed scenarios as $S'(z)$ for the thinning function and $A'(z)$ for the accumulation rate. The required reduction of the accumulation rate is $\approx 10\%$ at 8ky b2k and $\approx 15\%$ at the time of the Younger–Dryas stadial.

A similar correction in accumulation rate for the NorthGRIP site has been proposed for Marine Isotope Stage 3 (MIS–3) by Huber et al. (2006). A reduction by $\approx 25\%$ is required in order to eliminate the discrepancy between the output of a firn densification/gas fractionation model and $\delta^{15}\mathrm{N}$ measurements over the sequence of Interstadials 9–17. Similarly, Guillevic et al. (2013) require a 30% reduction on the accumulation rate as derived by a D–J ice flow model for the NEEM site tuned to the GICC05 chronology on a gas fractionation study focusing on Interstadials 8–10. In combination with these results, our study indicates an inadequacy of the D–J ice flow model in accurately reconstructing the strain and accumulation rate histories of the NorthGRIP and NEEM sites. In a synthesis of their results with the study of Landais et al. (2004, 2005) , Guillevic et al. (2013) propose that this possible inadequacy applies only for glacial conditions, but not for interglacial periods as well as glacial inceptions. In contrast, our study demonstrates how the D–J model fails to accurately estimate the accumulation rate history for the time span of the Holocene epoch with an error that is increasing as one approaches glacial conditions. Preliminary results we have, indicate that this error converges to a value of approximately 25% at a depth of 2100 m (≈ 40.2ky b2k). However, due to the ice diffusion length increasing with depth, inference of past temperatures below the depth of $\approx 2000\mathrm{m}$ comes with much greater uncertainty.

One of the possible explanations for the observed error is the use of a constant value used for the kink height $\mathcal{H}$ in the D–J ice flow model. This is the height that defines the shape of the horizontal velocity $v_x(z)$. Above $\mathcal{H}$, v_x is assumed to be constant and independent of z. Below $\mathcal{H}$, v_x is assumed to linearly decrease until the value of basal sliding velocity (Dansgaard and Johnsen, 1969). The choice of a constant value for $\mathcal{H}$ constitutes an oversimplification. Measurements of inclination in the bore–holes of the Dye–3 and Camp Century sites, reveal an enhanced deformation of the ice below $\mathcal{H}$ (Hansen and Gundestrup, 1988; Gundestrup et al., 1993). The estimated horizontal velocity profiles from those measurements demonstrate two things. First, an apparent kink in the estimated v_x profile is observed at the transition between the Holocene and glacial ice. Second, v_x deviates from the assumed constant value already above $\mathcal{H}$ (Fig. 7 and 8 in Hansen and Gundestrup (1988) and Gundestrup et al. (1993)) respectively. These two observations support the theory of a moving kink as also suggested by Guillevic et al. (2013). It is possible that the kink moves along with the interface between Holocene and glacial ice owing to the strong gradient in shear strain rates between the two materials. The latter is shown to be dependent on the ice fabric, impurity content and grain size of the ice (Paterson, 1991; Thorsteinsson et al., 1999; Cuffey et al., 2000). Additionally a concern can be raised regarding the validity of the assumption of the constant horizontal velocity from the kink height to the surface. We believe that implementations of ice flow models that take into account the aforementioned issues can likely provide better estimates of the ice thinning function and consequently past accumulation rates.

Furthermore, an additional effect that may have an impact on the accuracy of the thinning function estimation by means of a D–J model concerns possible migrations of the ice divide in the past. Previous studies have demonstrated that such effects have occurred at the Siple Dome (Nereson et al., 1998) and the Greenland summit (Marshall and Cuffey, 2000) ice core sites. Despite the uncertainty involved in the modeling efforts

addressing the problem of migrating ice divides, it is safe to assume that the Greenland Ice Sheet was very different during glacial times. For that reason one can expect that a simple ice flow model is very likely to present inaccuracies regarding the calculated strain rate history of the NorthGRIP site.

C. On the Holocene climate variability

An interesting feature of the diffusion derived temperature history is the observed Holocene variability. The 200y and 1ky low–pass filtered temperature signals in Fig. 6 reveal a climate variability on both millennial and centennial time scales. It can be seen in the 1 ky filtered curve (dark blue in Fig.6), that the cooling trend that started after the Holocene optimum persists through the Holocene and it intensifies at around 4 ky b2k, signifying a shift to cooler temperatures. In fact, a look into the 200 y low-pass filtered curve (light blue in Fig.6) reveals a warm event preceding the shift to cooler temperatures and giving rise to a mid-Holocene optimum. Signals indicative of a Roman and Medieval warm period are also present in the reconstruction. The manifest cold conditions between 300y and 800y b2k can be associated with the Little Ice Age, while a reversal towards warmer conditions cannot be robustly concluded from 200y b2k on.

An analysis of the derived Holocene climate variability based on the firn diffusion reconstruction is not a goal of this study. The several observable features of the temperature history possibly resemble climatic events documented by other proxies. In our view, the climatic shift at around 4ky b2k is a very interesting one. It possibly indicates that traces of the 4.2ky climatic event, observed in a wide range of sites (Staubwasser and Weiss, 2006; Fisher et al., 2008; Berkelhammer et al., 2012; Walker et al., 2012) at low mid and high latitudes, can also be found on the Greenland Ice Sheet. The high magnitude and rapid timing for parts of the temperature history in this study, point to the necessity for a more thorough assessment of the Holocene epoch by means of the the new water isotope diffusion method. The recently drilled and currently analyzed at a high resolution NEEM ice core (NEEM community members, 2013) can constitute an excellent dataset for such a study. Dual δ^{18}O and δD measurements on this high resolution sample set will also allow for a further investigation and application of the differential diffusion method as introduced in Johnsen et al. (2000) and applied in the works of Simonsen et al. (2011) and Gkinis (2011).

VII. Conclusions and outlook

Based on a high resolution δ^{18}O record from NorthGRIP, Greenland we estimated the diffusion length history for the site. By using a coupled water isotope diffusion and firn densification model, in combination with the GICC05 chronology and an estimate of the total thinning function obtained with a D–J ice flow model, we reconstructed a temperature history for that period 250–16,000y b2k. We outlined the technicalities regarding the implementation of the model as well as the spectral based estimation of the diffusion length from the high resolution record. Based on a sensitivity study we estimated the 1σ uncertainty of the reconstructed temperature to be approximately 2.5 K.

The inferred temperature history shows the climatic transition from the Last Glacial to the Holocene Optimum and the Holocene cooling trend thereafter. The BA and YD climatic transitions are present in the record, with a timing and amplitude that is broadly consistent with previous estimates obtained with gas isotopic fractionation methods. A cooling event with a duration of approximately 500 years and an amplitude of 5 K is observed in the early Holocene. It marks a possible relationship with signals of similar nature from other north high latitude as well as monsoon sites at approximately 8.5 ky b2k.

An overestimation of the temperature of the Holocene Climatic Optimum points to the necessity for a correction of the total thinning function. Assuming that the layer counted chronology is accurate, this correction would require a reduction of the accumulation rate of the order of 10% at 8ky b2k with respect to the level estimated with the D–J ice flow model. We discussed this result with respect to recent (Guillevic et al., 2013) as well as earlier (Huber et al., 2006) findings based on δ^{15}N studies that propose a similar reduction for Interstadials 9–17 and MIS–3 from the NEEM and NorthGRIP ice core respectively. We also proposed possible reasons for this discrepancy related to the fixed value of the kink height in the D–J model as well as probable past ice divide migrations.

We believe that the climate variability of our record, spanning millennial to centennial scales, is of particular interest and therefore requires further analysis, possibly additional evidence from other ice cores from the Greenland Ice Sheet and obviously careful comparisons with reconstructions based on other proxies from low, mid and especially high latitudes. The NEEM ice core can potentially provide an excellent record for that need, especially when considering the application of recently developed continuous infrared techniques (Gkinis et al.,

2011) that provide high resolution and precision δD and δ^{18}O datasets. Our future study objectives will revolve around these topics, not only within the scope of studying the past climate during the Holocene epoch, but also within the scope of understanding the mechanisms that affect the responsivity of the δ^{18}O signal to a set of input climatic parameters, most notably temperature and furthermore result in a poor (almost absent) signal to noise ratio during a period that has likely seen sizable climatic variations.

Acknowledgements

IRMS analysis was performed by Anita Boas. We would like to thank Eric Steig, Christo Buizert, and Takuro Kobashi for fruitful discussions. We acknowledge funding through NSF Award ARC 0806387 and the Lundbek foundation. The NorthGRIP project is directed and organised by the Department of Geophysics at the Niels Bohr Institute for Astronomy, Physics and Geophysics, University of Copenhagen. It was being supported by the National Science Foundations of Denmark, Belgium, France, Germany, Iceland, Japan, Sweden, Switzerland and the United States of America. This work would not have been possible without the insight and innovative mind of Sigfus J. Johnsen.

References

Abramowitz, M., Stegun, I. A., 1964. Handbook of Mathematical Functions with Formulas, Graphs, and Mathematical Tables, ninth Dover printing, Edition. Dover, New York.

Alley, R. B., Bolzan, J. F., Whillans, I., 1982. Polar firn densification and grain growth. Annals Of Glaciology 3, 7–11.

Alley, R. B., Mayewski, P. A., Sowers, T., Stuiver, M., Taylor, K. C., Clark, P. U., Jun. 1997. Holocene climatic instability: A prominent, widespread event 8200 yr ago. Geology 25 (6), 483–486.

Andersen, K. K., Ditlevsen, P. D., Rasmussen, S. O., Clausen, H. B., Vinther, B. M., Johnsen, S. J., Steffensen, J. P., Aug. 2006. Retrieving a common accumulation record from Greenland ice cores for the past 1800 years. Journal Of Geophysical Research-Atmospheres 111 (D15), D15106.

Andersen, N., 1974. Calculation of filter coefficients for Maximum Entropy spectral analysis. Geophysics 39 (1), 69–72.

Andrews, J. T., Keigwin, L., Hall, F., Jennings, A. E., Aug. 1999. Abrupt deglaciation events and Holocene palaeoceanography from high-resolution cores, Cartwright Saddle, Labrador Shelf, Canada. Journal of Quaternary Science 14 (5), 383–397.

Berkelhammer, M., Sinha, A., Stott, L., Cheng, H., Pausata, F. S. R., Yoshimura, K., 2012. An abrupt shift in the Indian Monsoon 4000 years ago. In: Geophys. Monogr. Ser. Vol. 198. AGU, Washington, DC, pp. 75–87.

Bond, G., Kromer, B., Beer, J., Muscheler, R., Evans, M. N., Showers, W., Hoffmann, S., Lotti-Bond, R., Hajdas, I., Bonani, G., Dec. 2001. Persistent solar influence on North Atlantic climate during the Holocene. Science 294 (5549), 2130–2136.

Cuffey, K. M., Alley, R. B., Grootes, P. M., Bolzan, J. M., Anandakrishnan, S., 1994. Calibration of the δ^{18}O isotopic paleothermometer for central Greenland, using borehole temperatures. Journal Of Glaciology 40 (135), 341–349.

Cuffey, K. M., Clow, G. D., Alley, R. B., Stuiver, M., Waddington, E., Saltrus, R. W., Oct. 1995. Large Arctic temperature-change at the Wisconsin-Holocene glacial transition. Science 270 (5235), 455–458.

Cuffey, K. M., Thorsteinsson, T., Waddington, E. D., Dec. 2000. A renewed argument for crystal size control of ice sheet strain rates. Journal of Geophysical Research-solid Earth 105 (B12), 27889–27894.

Dahl-Jensen, D., Gundestrup, N., Gogineni, S. P., Miller, H., 2003. Basal melt at NorthGrip modeled from borehole, ice-core and radio-echo sounder observations. Annals of Glaciology, Vol 37 37, 207–212.

Dahl Jensen, D., Mosegaard, K., Gundestrup, N., Clow, G. D., Johnsen, S. J., Hansen, A. W., Balling, N., Oct. 1998. Past temperatures directly from the Greenland ice sheet. Science 282 (5387), 268–271.

Dalfes, H., Kukla, G., Weiss, H. (Eds.), 1997. Third millennium BC climate change and old world collapse. Vol. 49. NATO ASI Ser. 1, Springer, New York.

Dansgaard, W., 1964. Stable isotopes in precipitation. Tellus 16 (4), 436–468.

Dansgaard, W., Johnsen, S. J., 1969. A flow model and a time scale for the ice core from Camp Century, Greenland. Journal of Glaciology 8 (53), 215–223.

deMenocal, P. B., Apr. 2001. Cultural responses to climate change during the late Holocene. Science 292 (5517), 667–673.

Denton, G. H., Karlen, W., 1973. Holocene climatic variations. their pattern and possible cause. Quaternary Research 3 (2), 155 – 205.

Ellison, C. R. W., Chapman, M. R., Hall, I. R., Jun. 2006. Surface and deep ocean interactions during the cold climate event 8200 years ago. Science 312 (5782), 1929–1932.

Epstein, S. Mayeda, T., 1953. Variations of ^{18}O content of waters from natural sources. Geochimica Cosmochimica Acta 4, 213?224.

Fisher, D., Osterberg, E., Dyke, A., Dahl-Jensen, D., Demuth, M., Zdanowicz, C., Bourgeois, J., Koerner, R. M., Mayewski, P., Wake, C., Kreutz, K., Steig, E., Zheng, J., Yalcin, K., Goto-Azuma, K., Luckman, B., Rupper, S., Aug. 2008. The Mt Logan Holocene-late Wisconsinan isotope record: Tropical pacific-yukon connections. Holocene 18 (5), 667–677.

Gasse, F., Jan. 2000. Hydrological changes in the African tropics since the last glacial maximum. Quaternary Science Reviews 19 (1-5), 189–211.

Gkinis, V., 2011. High resolution water isotope data from ice cores. Ph.D. thesis, Niels Bohr Institute, University of Copenhagen.

Gkinis, V., Popp, T. J., Blunier, T., Bigler, M., Schupbach, S., Kettner, E., Johnsen, S. J., 2011. Water isotopic ratios from a continuously melted ice core sample. Atmospheric Measurement Techniques 4 (11), 2531–2542.

Goujon, C., Barnola, J. M., Ritz, C., Dec. 2003. Modeling the densification of polar firn including heat diffusion: Application to close-off characteristics and gas isotopic fractionation for antarctica and greenland sites. Journal Of Geophysical Research-Atmospheres 108 (D24), 4792.

Grachev, A. M., Severinghaus, J. P., Mar. 2005. A revised +10 +/- 4 degrees C magnitude of the abrupt change in Greenland temperature at the younger dryas termination using published Gisp2 gas isotope data and air thermal diffusion constants. Quaternary Science Reviews 24 (5-6), 513–519.

Guillevic, M., Bazin, L., Landais, A., Kindler, P., Orsi, A., Masson-Delmotte, V., Blunier, T., Buchardt, S. L., Capron, E., Leuenberger, M., Martinerie, P., Prié, F., Vinther, B. M., 2013. Spatial gradients of temperature, accumulation and δ^{18}O-ice in Greenland over a series of Dansgaard–Oeschger events. Climate of the Past 9 (3), 1029–1051.

Gundestrup, N. S., Dahl-Jensen, D., Hansen, B. L., Kelty, J., 1993. Bore-hole survey at Camp Century, 1989. Cold Regions Science and Technology 21 (2), 187–193.

Gupta, A. K., Anderson, D. M., Overpeck, J. T., Jan. 2003. Abrupt changes in the asian southwest monsoon during the Holocene and their links to the north atlantic ocean. Nature 421 (6921), 354–357.

Hansen, B. L., Gundestrup, N. S., 1988. Resurvey of bore hole at Dye-3, south Greenland. Journal of Glaciology 34 (117), 178–182.

Haug, G. H., Hughen, K. A., Sigman, D. M., Peterson, L. C., Rohl, U., Aug. 2001. Southward migration of the intertropical convergence zone through the Holocene. Science 293 (5533), 1304–1308.

Hayes, M. H., 1996. Statistical digital signal processing and modeling. John Wiley & Sons.

Herron, M. M., Langway, C. C., 1980. Firn densification - an empirical-model. Journal Of Glaciology 25 (93), 373–385.

Huber, C., Leuenberger, M., Spahni, R., Fluckiger, J., Schwander, J., Stocker, T. F., Johnsen, S., Landals, A., Jouzel, J., Mar. 2006. Isotope calibrated Greenland temperature record over Marine Isotope Stage 3 and its relation to CH_4. Earth and Planetary Science Letters 243 (3-4), 504–519.

Jean-Baptiste, P., Jouzel, J., Stievenard, M., Ciais, P., May 1998. Experimental determination of the diffusion rate of deuterated water vapor in ice and application to the stable isotopes smoothing of ice cores. Earth And Planetary Science Letters 158 (1-2), 81–90.

Johnsen, S. J., 1977. Stable isotope homogenization of polar firn and ice. Isotopes and impurities in snow and ice, 210–219.

Johnsen, S. J., Clausen, H. B., Cuffey, K. M., Hoffmann, G., Schwander, J., Creyts, T., 2000. Diffusion of stable isotopes in polar firn and ice. the isotope effect in firn diffusion. In: Hondoh, T. (Ed.), Physics of Ice Core Records. Hokkaido University Press, Sapporo, pp. 121–140.

Johnsen, S. J., Dahl Jensen, D., Dansgaard, W., Gundestrup, N., Nov. 1995. Greenland paleotemperatures derived from grip bore hole temperature and ice core isotope profiles. Tellus Series B-Chemical And Physical Meteorology 47 (5), 624–629.

Johnsen, S. J., DahlJensen, D., Gundestrup, N., Steffensen, J. P., Clausen, H. B., Miller, H., Masson-Delmotte, V., Sveinbjornsdottir, A. E., White, J., 2001. Oxygen isotope and palaeotemperature records from six Greenland ice-core stations: Camp Century, Dye-3, GRIP, GISP2, Renland and NorthGrip. Journal Of Quaternary Science 16 (4), 299–307.

Johnsen, S. J., Dansgaard, W., White, J. W. C., 1989. The origin of arctic precipitation under present and glacial conditions. Tellus 41B, 452–468.

Jouzel, J., Alley, R. B., Cuffey, K. M., Dansgaard, W., Grootes, P., Hoffmann, G., Johnsen, S. J., Koster, R. D., Peel, D., Shuman, C. A., Stievenard, M., Stuiver, M., White, J., 1997. Validity of the temperature reconstruction from water isotopes in ice cores. Journal Of Geophysical Research-Oceans 102 (C12), 26471–26487.

Jouzel, J., Merlivat, L., 1984. Deuterium and oxygen 18 in precipitation: modeling of the isotopic effects during snow formation. Journal of Geophysical Research-Atmospheres 89 (D7), 11749 – 11759.

Kay, S. M., Marple, S. L., 1981. Spectrum analysis - a

modern perspective. Proceedings Of The Ieee 69 (11), 1380–1419.

Kobashi, T., Kawamura, K., Severinghaus, J. P., Barnola, J. M., Nakaegawa, T., Vinther, B. M., Johnsen, S. J., Box, J. E., Nov. 2011. High variability of Greenland surface temperature over the past 4000 years estimated from trapped air in an ice core. Geophysical Research Letters 38, L21501.

Landais, A., Barnola, J. M., Masson-Delmotte, V., Jouzel, J., Chappellaz, J., Caillon, N., Huber, C., Leuenberger, M., Johnsen, S. J., 2004. A continuous record of temperature evolution over a sequence of Dansgaard-Oeschger events during Marine Isotopic Stage 4 (76 to 62 kyr bp). Geophysical Research Letters 31 (22), L22211.

Landais, A., Jouzel, J., Masson-Delmotte, V., Caillon, N., 2005. Large temperature variations over rapid climatic events in Greenland: a method based on air isotopic measurements. Comptes Rendus Geoscience 337 (10-11), 947–956.

Lang, C., Leuenberger, M., Schwander, J., Johnsen, S., 1999. 16C rapid temperature variation in central Greenland 70,000 years ago. Science 286 (5441), 934–937.

Lorius, C., Merlivat, L., Hagenmann, R., 1969. Variation in mean Deuterium content of precipitations in Antarctica. Journal of Geophysical Research 74 (28), 7027–7030.

Marshall, S. J., Cuffey, K. M., Jun. 2000. Peregrinations of the Greenland ice sheet divide in the last glacial cycle: implications for central Greenland ice cores. Earth and Planetary Science Letters 179 (1), 73–90.

NGRIP members, 2004. High-resolution record of northern hemisphere climate extending into the last interglacial period. Nature 431 (7005), 147–151.

Mook, W., 2000. Environmental Isotopes in the Hydrological Cycle: Principles and Applications, vol. I, IAEA. Unesco and IAEA.

NEEM community members, 2013. Eemian interglacial reconstructed from a Greenland folded ice core. Nature 493 (7433), 489–494.

Nereson, N. A., Raymond, C. F., Waddington, E. D., Jacobel, R. W., 1998. Migration of the Siple Dome ice divide, West Antarctica. Journal of Glaciology 44 (148), 643–652.

Paterson, W. S. B., Nov. 1991. Why ice-age ice is sometimes soft. Cold Regions Science and Technology 20 (1), 75–98.

Ramseier, R. O., 1967. Self-diffusion of tritium in natural and synthetic ice monocrystals. Journal Of Applied Physics 38 (6), 2553–2556.

Rasmussen, S. O., Andersen, K. K., Svensson, A. M., Steffensen, J. P., Vinther, B. M., Clausen, H. B., Siggaard-Andersen, M. L., Johnsen, S. J., Larsen, L. B., Dahl-Jensen, D., Bigler, M., Rothlisberger, R., Fischer, H., Goto-Azuma, K., Hansson, M. E., Ruth, U., Mar. 2006. A new Greenland ice core chronology for the last glacial termination. Journal Of Geophysical Research-Atmospheres 111 (D6), 10.1029/2005JD006079.

Risebrobakken, B., Jansen, E., Andersson, C., Mjelde, E., Hevroy, K., Mar. 2003. A high-resolution study of Holocene paleoclimatic and paleoceanographic changes in the nordic seas. Paleoceanography 18 (1), 1017.

Rohling, E. J., Palike, H., Apr. 2005. Centennial-scale climate cooling with a sudden cold event around 8,200 years ago. Nature 434 (7036), 975–979.

Schwander, J., Sowers, T., Barnola, J. M., Blunier, T., Fuchs, A., Malaize, B., Aug. 1997. Age scale of the air in the summit ice: Implication for glacial-interglacial temperature change. Journal Of Geophysical Research-Atmospheres 102 (D16), 19483–19493.

Severinghaus, J. P., Brook, E. J., Oct. 1999. Abrupt climate change at the end of the last glacial period inferred from trapped air in polar ice. Science 286 (5441), 930–934.

Severinghaus, J. P., Sowers, T., Brook, E. J., Alley, R. B., Bender, M. L., 1998. Timing of abrupt climate change at the end of the Younger-Dryas interval from thermally fractionated gases in polar ice. Nature 391 (6663), 141–146.

Simonsen, S. B., Johnsen, S. J., Popp, T. J., Vinther, B. M., Gkinis, V., Steen-Larsen, H. C., 2011. Past surface temperatures at the NorthGrip drill site from the difference in firn diffusion of water isotopes. Climate of the Past 7 (4), 1327–1335.

Staubwasser, M., Weiss, H., Nov. 2006. Holocene climate and cultural evolution in late prehistoric-early historic west asia - introduction. Quaternary Research 66 (3), 372–387.

Svensson, A., Andersen, K. K., Bigler, M., Clausen, H. B., Dahl-Jensen, D., Davies, S. M., Johnsen, S. J., Muscheler, R., Parrenin, F., Rasmussen, S. O., Roethlisberger, R., Seierstad, I., Steffensen, J. P., Vinther, B. M., 2008. A 60,000 year Greenland stratigraphic ice core chronology. Climate of the Past 4 (1), 47–57.

Thorsteinsson, T., Waddington, E. D., Taylor, K. C., Alley, R. B., Blankenship, D. D., 1999. Strain-rate enhancement at Dye 3, Greenland. Journal of Glaciology 45 (150), 338–345.

Van der Wel, L. G., Gkinis, V., Pohjola, V. A., Meijer, H. A. J., 2011. Snow isotope diffusion rates measured in a laboratory experiment. Journal of Glaciology 57 (201),

30–38.

Vinther, B. M., Buchardt, S. L., Clausen, H. B., Dahl-Jensen, D., Johnsen, S. J., Fisher, D. A., Koerner, R. M., Raynaud, D., Lipenkov, V., Andersen, K. K., Blunier, T., Rasmussen, S. O., Steffensen, J. P., Svensson, A. M., 2009. Holocene thinning of the Greenland ice sheet. Nature 461 (7262), 385–388.

Vinther, B. M., Clausen, H. B., Johnsen, S. J., Rasmussen, S. O., Andersen, K. K., Buchardt, S. L., Dahl-Jensen, D., Seierstad, I. K., Siggaard-Andersen, M. L., Steffensen, J. P., Svensson, A., Olsen, J., Heinemeier, J., 2006. A synchronized dating of three Greenland ice cores throughout the Holocene. Journal Of Geophysical Research-Atmospheres 111 (D13), D13102.

Walker, M. J. C., Berkelhammer, M., Bjorck, S.rck, S., Cwynar, L. C., Fisher, D. A., Long, A. J., Lowe, J. J., Newnham, R. M., Rasmussen, S. O., Weiss, H., 2012. Formal subdivision of the Holocene series/epoch: a discussion paper by a working group of INTIMATE (integration of ice-core, marine and terrestrial records) and the subcommission on quaternary stratigraphy (international commission on stratigraphy). Journal of Quaternary Science 27 (7), 649–659.

Wang, Y. J., Cheng, H., Edwards, R. L., He, Y. Q., Kong, X. G., An, Z. S., Wu, J. Y., Kelly, M. J., Dykoski, C. A., Li, X. D., May 2005. The Holocene Asian monsoon: Links to solar changes and north atlantic climate. Science 308 (5723), 854–857.

Weiss, H., Bradley, R. S., Jan. 2001. Archaeology - what drives societal collapse? Science 291 (5504), 609–610.

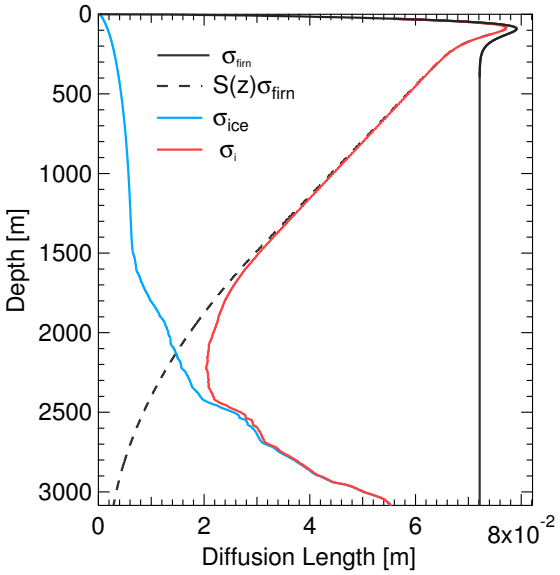

Fig. 1. Vertical profiles of $\sigma_{\rm firn}$, $S(z)\sigma_{\rm firn}$, $\sigma_{\rm ice}$ and σ_i For the calculation of $\sigma_{\rm firn}$ the parameters we used for the H–L model were: $P = 0.7$ Atm, $\rho_0 = 330$ kgm^{-3}, $\rho_{\rm CO} = 804.3$ kgm^{-3}, $T = 242.15$ K, and $A = 0.2$ myr^{-1} ice equivalent.

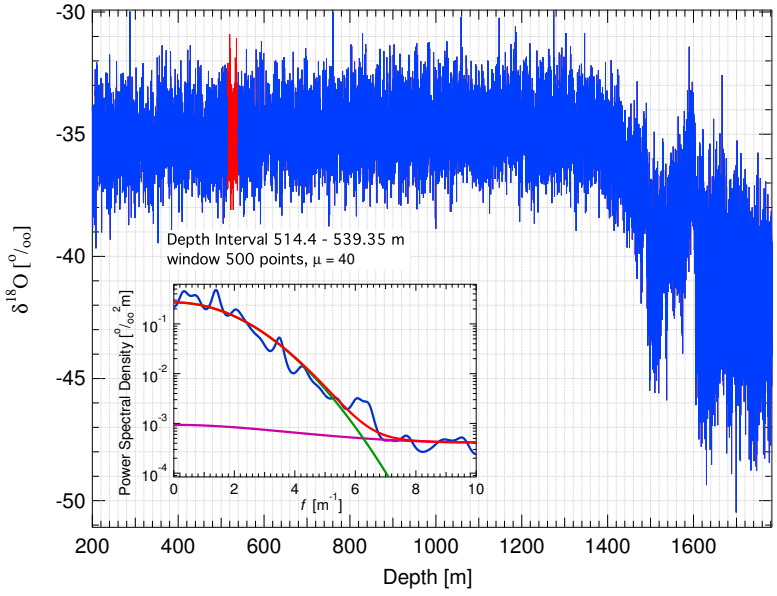

Fig. 2. NorthGRIP high resolution (0.05 m) δ^{18}O record. The subplot is an example of a power spectral density estimation with the MEM (blue curve). The length of the window is 500 points and the order of the AR model for the spectral estimation is $\mu = 40$. The model for the spectral density P_s is presented in red, $|\hat{\eta}(k)|^2$ is shown in purple and P_σ in green.

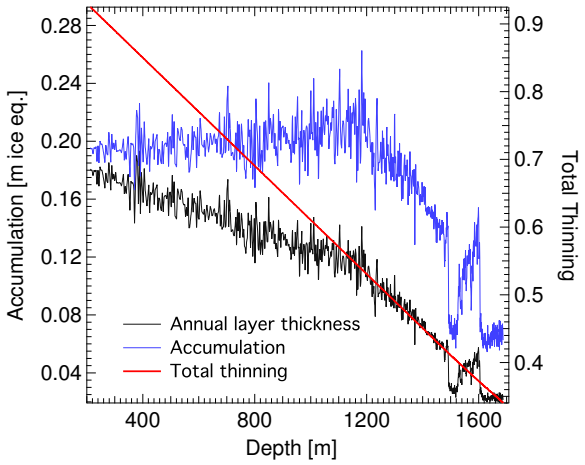

Fig. 3. Annual layer thickness, total thinning and accumulation rate for NorthGRIP based on the GICC05 chronology and a 1–D Dansgaard–Johnsen ice flow model

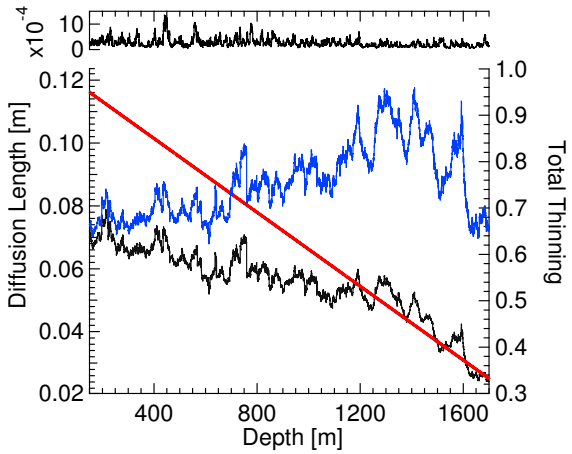

Fig. 4. Results of the diffusion length estimation. Bottom plot: raw diffusion length values $\sigma_{\mathrm{i}}^2(z)$ (bottom black curve) and $\sigma_{\mathrm{firn}}^2(z)$ (blue curve) after correcting for total thinning (red curve) and σ_{ice}^2 Top plot: Standard deviation of the 41 estimates of the diffusion length for every depth in m ice eq.

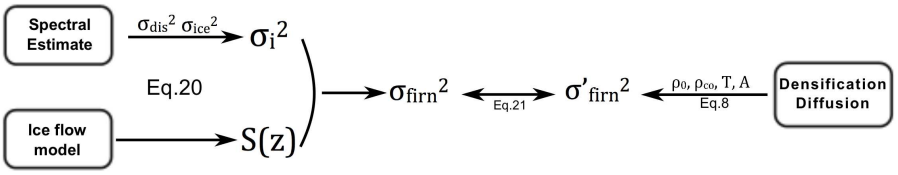

Fig. 5. Block diagram of the computation scheme for the temperature reconstruction. Data-based estimates of the σ_{firn}^2 parameter are obtained from the spectral estimation procedure and then corrected for discrete sampling, ice diffusion and ice flow thinning effects. A model based estimate of the diffusion length $\sigma_{\mathrm{firn}}^{\prime 2}$ using an isothermal firn layer of temperature T and accumulation A is obtained using the densification/diffusion calculation. Finally we compute roots of the term $\sigma_{\mathrm{firn}}^{\prime 2} - \sigma_{\mathrm{firn}}^2$ using T as the independent variable.

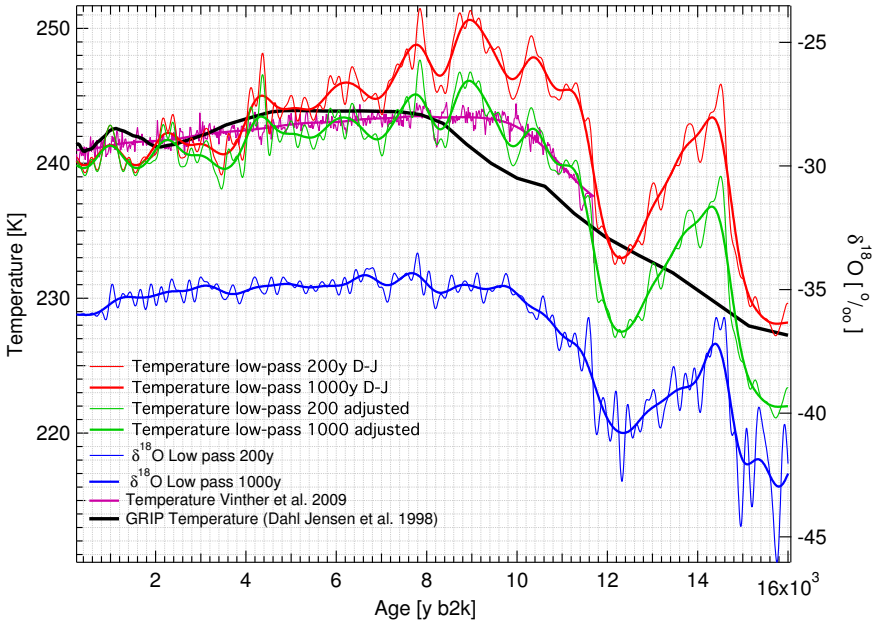

Fig. 6. The old (red) and updated (green) temperature reconstruction using the proposed thinning function $S'(z)$. The signal is filtered by applying a low pass filter with a cut–off at 1ky (thick lines) and 200y (thin lines). In blue we present the low–pass filtered δ^{18}O signal with a cut–off at 1ky (thick line) and 200y (thin line) In purple we plot the temperature reconstruction from Vinther et al. (2009) where an offset of 239K has been added.

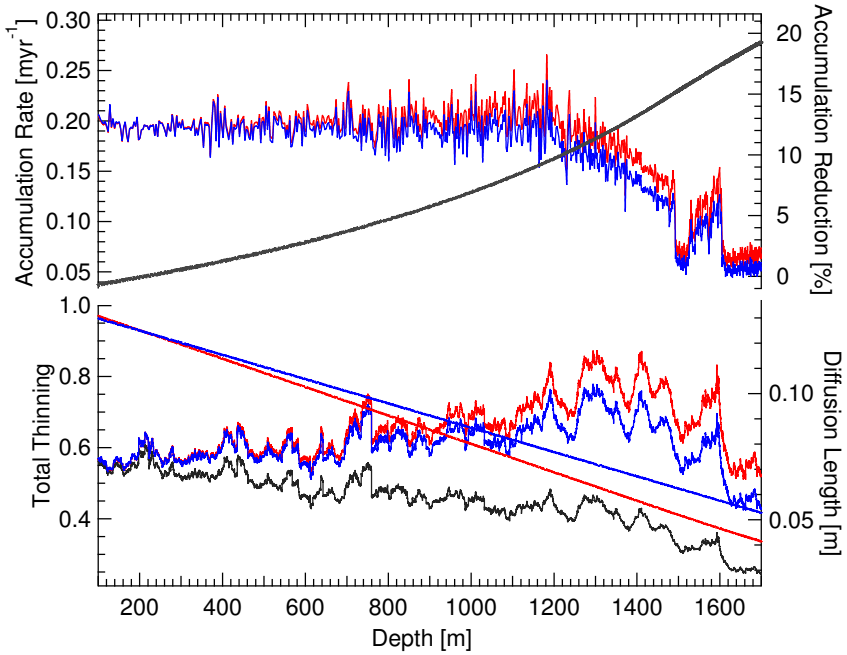

Fig. 7. The old (red) and new proposed (blue) accumulation rate ($A(z)$, $A'(z)$) and thinning history ($S(z)$, $S'(z)$) for the North GRIP site based on the tuning of the Holocene optimum signal at 8ky b2k to 3 K with respect to the level of 225 y b2k. With the dark gray line we illustrate the % proposed reduction in accumulation rates. At the bottom graph the black curve presents the raw diffusion length signal $\sigma_i\,(z)$. Accounting for the two different scenarios of the thinning function $S\,(z)$ and $S'\,(z)$ we obtain the red (old) and blue (updated) curve for $\sigma_{\rm firn}\,(z)$ and $\sigma'_{\rm firn}\,(z)$